

# Displacement power spectrum measurement of a macroscopic optomechanical system at thermal equilibrium

A. Di Virgilio<sup>1</sup>, L. Barsotti<sup>1</sup>, S. Braccini<sup>1</sup>, C. Bradaschia<sup>1</sup>, G. Cella<sup>1</sup>, V. Dattilo <sup>2</sup>, M. Del Prete<sup>1</sup>, I. Ferrante<sup>3</sup>, F. Fidecaro<sup>3</sup>, I. Fiori<sup>1</sup>, F. Frasconi<sup>1</sup>, A. Gennai<sup>1</sup>, A. Giazotto<sup>1</sup>, P. La Penna<sup>2</sup>, G. Losurdo <sup>4</sup>, E. Majorana<sup>5</sup>, M. Mantovani <sup>6</sup>, F. Paoletti<sup>1,2</sup>, R. Passaquieti<sup>3</sup>, D. Passuello<sup>1</sup>, F. Piergiovanni<sup>7</sup>, A. Porzio<sup>8</sup>, P. Puppo<sup>5</sup>, F. Raffaelli<sup>1</sup>, P. Rapagnani<sup>5</sup>, F. Ricci<sup>5</sup>, S. Solimeno<sup>8,9</sup>, G. Vajente<sup>1,10</sup>, F. Vetrano<sup>7</sup>

<sup>1</sup>INFN, Sez. di Pisa, Pisa, Italy

<sup>2</sup>EGO, European Gravitational Observatory, Cascina (Pi)

<sup>3</sup>Università' di Pisa, Italy

<sup>4</sup>INFN Sezione di Firenze, Sesto Fiorentino, Italy

<sup>5</sup>Università di Roma1, and INFN-Roma1, Roma Italy

<sup>6</sup>Università' di Siena, Italy

<sup>7</sup>Università di Urbino, Urbino, Italy

<sup>8</sup>Coherentia, CNR-INFM, and CNISM Unitá di Napoli

<sup>9</sup>INFN, Sez. di Napoli, Università di Napoli

<sup>10</sup>Scuola Normale Superiore, Pisa

(Dated: May 26, 2019)

The mirror relative motion of a suspended Fabry-Perot cavity is studied in the frequency range 3–100 Hz. The experimental measurements presented in this paper, have been performed at the Low Frequency Facility, a high finesse optical cavity 1 cm long suspended to a mechanical seismic isolation system identical to that one used in the VIRGO experiment. The measured relative displacement power spectrum is compatible with a system at thermal equilibrium within its environmental. In the frequency region above 3 Hz, where seismic noise contamination is negligible, the measurement distribution is stationary and Gaussian, as expected for a system at thermal equilibrium. Through a simple mechanical model it is shown that: applying the fluctuation dissipation theorem the measured power spectrum is reproduced below 90 Hz and noise induced by external sources are below the measurement.

PACS numbers:

## I. INTRODUCTION

Thermal fluctuations of mechanical systems are considered the most relevant limitation of ground based interferometers for gravitational waves detection in the low frequency region, where several gravitational wave signals are expected[1]. The statistical behavior is well described by the Fluctuation Dissipation Theorem (FDT), which states a general relationship between the response of a given system to an external disturbance and the internal fluctuation of the system in the absence of the disturbance. Such a response is characterized by a response function or equivalently by an admittance, or an impedance [2, 3, 4]. The test masses for gravitational wave interferometer are complex mechanical systems where contributions to the thermal noise come from different elements of the structure: the suspension wires of the mirror, the mirror bulk and the mirror coating, which is considered one of most severe thermal noise source for the present and near future detectors, just to mention a few of them. Measurements devoted to the evaluation of different dissipation mechanisms and of the parameters describing them, are often performed on resonance. Just a few experimental apparatus have been conceived to measure the thermal noise spectrum out of resonance and in the frequency region above 100 Hz [5, 6, 7, 8]. The Low Frequency Facility (LFF) is the

test bench on top of which the Italian R&D program of the VIRGO experiment is based on. Its main purpose is the relative displacement measurement of two suspended mirrors forming a high finesse Fabry-Perot cavity suspended from a seismic isolation system and the study of the thermal noise spectrum in the region starting from 10 Hz[9]. This is made possible by a Superattenuator (SA), very similar to the ones installed in VIRGO, at the INFN Pisa laboratory. Care has been used in designing and assembling this experiment in order to keep the experimental apparatus as close as possible to the VIRGO's suspensions. Moreover, since the seismic noise reduction to the payload level is very large, the LFF represents also an independent benchmark of the VIRGO suspension behavior in the low frequency region. Recently, data collected at the LFF has shown the presence of an optical spring due to the radiation pressure noise of the system [10]. Within the frequency band 3 – 90 Hz this thermal-noise dominated system is unique as well as the presence of the optical spring acting between two mirrors of the cavity. The first section of this paper shortly describes the experimental apparatus. An introduction of the mechanical model reproducing the experimental measurements is presented in the second section. Within the third section is focused on the evaluation of the main noise coming from external sources in LFF. In the last section, before the conclusions, a general overview on the

measured spectra is given, paying particular attention to the main characteristics of the thermal noise driven mechanisms. Then the absorption coefficients found fitting the data with the model are discussed. .

## II. THE EXPERIMENT SET-UP AND DATA ACQUISITION

The last stage of the experimental apparatus is sketched in fig. 1 while a more detailed description can be found in references [9]. The reflectivity, transmission and loss ( $R_i$ ,  $T_i$ ,  $A_i$  with  $i = 1, 2$  respectively) of the two mirrors used in our set-up are given in table I together with the nominal cavity finesse and the laser input power. RFC (reference cavity) and the suspended mirrors (enclosed in figure in grey boxes) are in vacuum.

$R_1$	0.9991
$R_2$	0.9999
$A_1$ and $A_2$	0.00001
$T_1$	0.0009
<i>Nominal Finesse</i>	6300
$P_{in}$	200 mW

TABLE I: Optical parameters of the cavity

The Finesse, estimated from the transmission profile of the uncontrolled cavity, is about  $5500 \pm 1500$ . The static radiation pressure force is about  $5 \mu N$ . The suspension system adopted to insulate from seismic noise the high finesse 1 cm long Fabry-Perot cavity is a single SA chain, equal to the ones of VIRGO interferometer test masses[4]. The suspension and the cavity are in vacuum inside a tank. The curved mirror is a 25 mm diameter mirror embedded in a large steel cylinder to form its holder and it plays the role of the VIRGO test mass (VM). The flat mirror of the cavity (AX, auxiliary mirror) is hung, by means of an independent three-stage suspension, to the last mechanical seismic filter of the chain called Filter7. It includes an intermediate mass  $m_d = 71.72$  kg and an additional smaller clamp of the AX suspension wire,  $m_t = 0.08$  kg. The control of the longitudinal motion is done by acting only on the VM mirror using the 2 coil-magnet pairs. This actuation technique is identical to the one implemented in the VIRGO interferometer [11, 12, 13] where the coils are screwed on the reference mass (RM) and the magnets are glued on the back side of the mirror holder. Fig. 1 shows the cavity, the input beam, the longitudinal control loop scheme and the acquired signals. The laser beam, phase modulated at 17 MHz and independently frequency stabilized on a 15 cm rigid ULE reference cavity, is injected into the cavity. The reflected power, deviated by the polarizer, is detected by a photodiode and demodulated by the mixer (Pound-Drever-Hall scheme, P-D-H), with a scheme analogous to the one used for the VIRGO pre-stabilization

circuit, which should provide a laser frequency stabilization at the  $mHz/\sqrt{Hz}$  level [14]. The linear zone of the read-out signal is about  $10^{-10} m$ . The feedback control loop is based on a Digital Sygnal Processor (DSP) developed for the VIRGO suspension system control. The cavity signal is amplified and then sent to a 16 bit ADC while the DSP takes care of the signal filtering to control the stability of the longitudinal electromechanical loop. The filtered signal is sent to four DAC (20 bit) channels and then to the four coil drivers. The error signal is acquired with a LabView program using a 16 bit ADC. Mixer output, coil voltage, filtered by an anti-aliasing filter at 3.4 kHz, are the relevant signal acquired during measurement, with acquisition rate of 400 Hz. They are indicated in fig. 1 as ERROR, COIL2 and PROBE.

## III. MEASUREMENTS AND MECHANICAL MODEL

In fig. 2 the power spectrum of the two mirrors relative motion suspended to the SA chain is shown. This plot has been obtained analysing a collected data stretch 1 hour long. A typical structure of the SA chain excited by the seismic noise is visible below 3 Hz while at higher frequency a few peaks with high mechanical quality factor (Q) are present. In particular, the broad peak coming from the optical spring at about 90 Hz is well visible. To better understand the behavior of the LFF experimental set-up, a one-dimensional model with mass-less wires and point-like masses has been developed. Although the SA chain adopted to isolate the optical components from seismic noise is a complex system, the mechanical model is confined to the study of the dynamical system formed by the two mechanical branches hung to the Filter7 (see fig. 1). Each branch includes one mirror of the optical cavity: the first one (AX) is made of four masses suspended in series while the second one (VM) is composed by a simple pendulum from which two elements are attached in parallel.

In Table II the mechanical parameters of the LFF model are collected.

The feedback loop circuit has been included within the model taking into account the filtering calculation performed by the DSP as well as the coil driver impedances (see fig. 1). The magnetic actuator coupling constant is  $\alpha = 3 mN/A$  while the typical gain of the optical read-out is  $1.56 \times 10^{10} V/m$ . The transfer function of the function running in the DSP consists of the sum of two pieces: one has a real pole at 0.5 Hz (with gain 13 at frequency zero), and the other a real zero at 30 Hz (with gain 5 at 750 Hz). The low frequency feedback gain is of the order of  $10^5 - 10^6$ , large enough to reduce the large motion of the mirror from a few microns down to  $10^{-11} m$ , well inside the linear region of the P-D-H signal.

The system is affected by different noise sources entering through different dissipation mechanism, fig. 3 shows the control loop, the acquired signals and the ex-

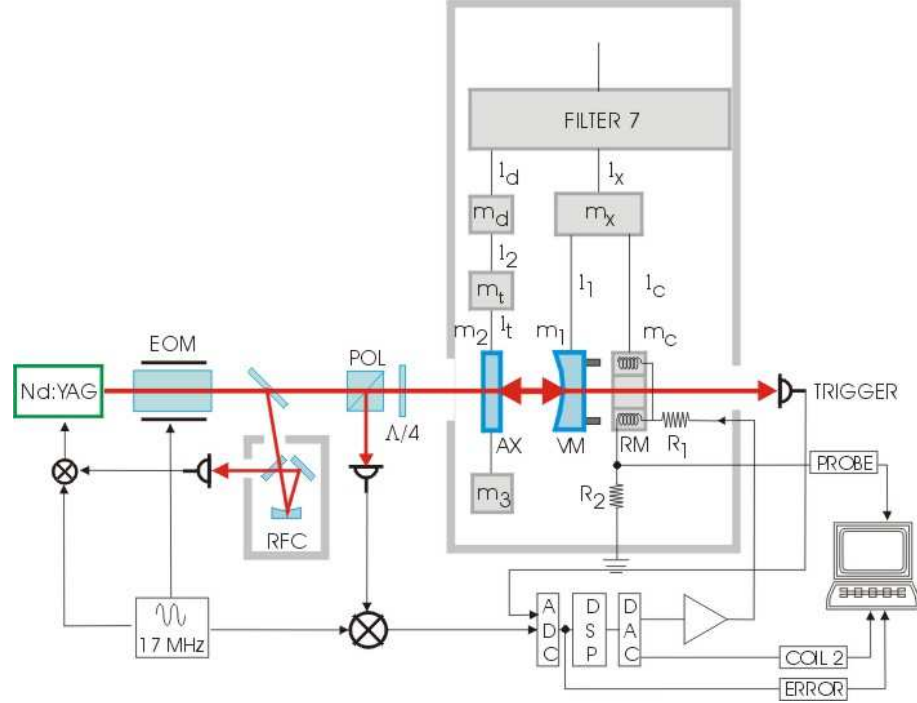


FIG. 1: Sketch of the experiment set-up from Filter7. The optical circuit, and the control loop are shown; gray boxes underline the components under vacuum.

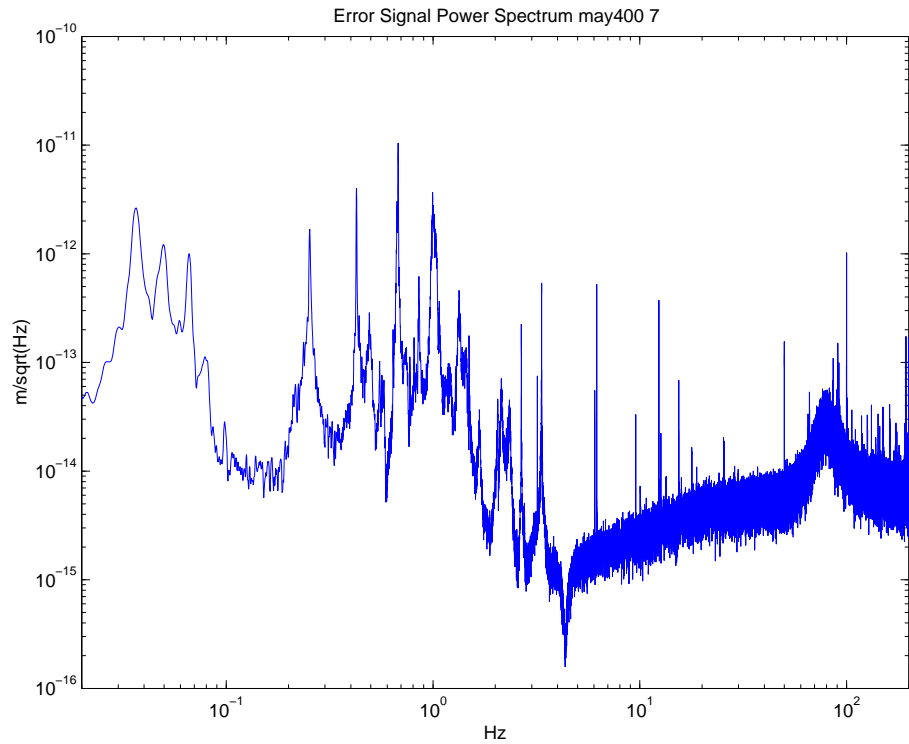


FIG. 2: Typical power spectrum of the relative motion of the suspended cavity, while the loop is active.

Masses	kg	Wires	mm
$m_d$	71.72	$l_d$	1100
$m_t$	0.08	$l_t$	250
$m_2$	0.296	$l_2$	500
$m_3$	2.5	$l_3$	300
$m_x$	80	$l_x$	1130
$m_1$	27.61	$l_1$	700
$m_c$	64.14	$l_c$	500

TABLE II: Mechanical characteristics of the LFF systems.

ternal noises entering in the system. This implies that the model should account for the possibility of changing the entering position of the noise sources (physically resembling the different sources affecting different stage of the electro-mechanical system). In particular, the critical points are suspension, mirror, electronic noise of the DSP and coil driver.

The thermal noise of a mechanical system can be calculated using the fluctuation dissipation theorem [2, 3]. The theorem defines a relation between the frequency distribution of thermal noise in a system and the mechanical admittance  $Y$ , which is the ratio between the resulting velocity and the applied force (i.e. the transfer function of the velocity as a function of the applied force):

$$Y(\omega) = \frac{v}{F} \quad (1)$$

Specifically, the displacement spectral density is given by:

$$x^2(\omega) = \frac{4k_B T}{\omega^2} \text{Real}(Y(\omega)) \quad (2)$$

where  $k_B$  is the Boltzmann's constant,  $T$  the temperature and  $Y$  the admittance,  $\omega = 2\pi\nu$ , where  $\nu$  is the frequency. In our case  $x$  is the distance from the resonance point of the cavity, as well as the relative motion of the two mirrors of the cavity, also called error signal of the feed-back longitudinal control loop. The model takes into account the rotational degree of freedom that can be excited by an off-axis beam, necessary since the beam hits the mirror few millimeters far from the center. This has been done by adding a single equation to the model, thus considering the flat mirror as a single oscillator of given momentum of inertia and a proper frequency around 3 Hz, as experimentally observed. This approximated models held because the proper frequencies of multi-pendulum suspension are well below the range analyzed in this context. The elastic constant of the rotation is 0.13 N/rad, with a inertial moment of the mirror  $3.2 \cdot 10^{-4} \text{ kgm}^2$ , the misalignment between the vertical rotational axis of the AX mirror and the point where the radiation pressure force is applied is 4 mm.

To take into account the losses we add inside the equation of motion a term proportional to the velocity (viscous damping) or we multiply the spring constants by  $(1 + i\phi)$  (structural damping), where  $\phi$  is the loss angle (usually considered constant and smaller than  $\phi = 10^{-4}$ ), [15, 16].

In the model only two dissipation terms have been considered: pure viscous damping acting on the longitudinal degree of freedom, and the other acting on the rotational one of the AX mirror. This simple choice is based on the fact that the AX pendulum has larger thermal noise, since its mass is 100 times lighter than the other. Moreover we can assess which dissipation mechanisms is dominant by analyzing the different frequency behavior, under the assumption that the absorption parameters are constant with the frequency.

Assuming that the control loop does not introduce noise [?], the model evaluates the thermal noise contribution to the relative motion  $x$  of the mirror of the cavity in the following way:

- in the open loop case, the mechanical impedance is evaluated by applying two equal and opposite forces to the two mirrors of the cavity, in the model the optical spring is described by a standard stiffness
- the thermal noise power spectrum of  $x$  is evaluated by using F-D-T
- the stochastic forces are evaluated by the thermal noise power spectrum of  $x$  and the model
- the closed loop motion, to be compared with the measurement, is evaluated by applying the thermal stochastic forces to the mirrors in the closed loop equations
- free parameters are the absorption coefficients and the optical spring stiffness, which are derived by fitting the data with the model.

Figure 4 shows the thermal noise spectra in the following cases: open loop with and without optical spring and the closed loop with optical spring (using the typical feed-back parameters used in the runs which have been analyzed).

#### IV. EXTERNAL NOISES CONTRIBUTIONS

Few peaks are evident in the spectrum: the 12 Hz peak is related to the existence of the small clamp  $m_t$ , all the others have not been identified. Some of the peaks are not stationary; comparing the data of two different time periods of a single acquisition run, it has been checked that the peak heights are enhanced while the noise floor remain unaffected [9]. For this reason those peaks are not crucial for the comprehension of the noise floor; they are related even to the excitation of degrees of freedom orthogonal to the longitudinal one, or through the input beam which is in air, or to spurious electromagnetic couplings.

In the following the measured power spectrum will be compared with all the external noise sources. Thanks to

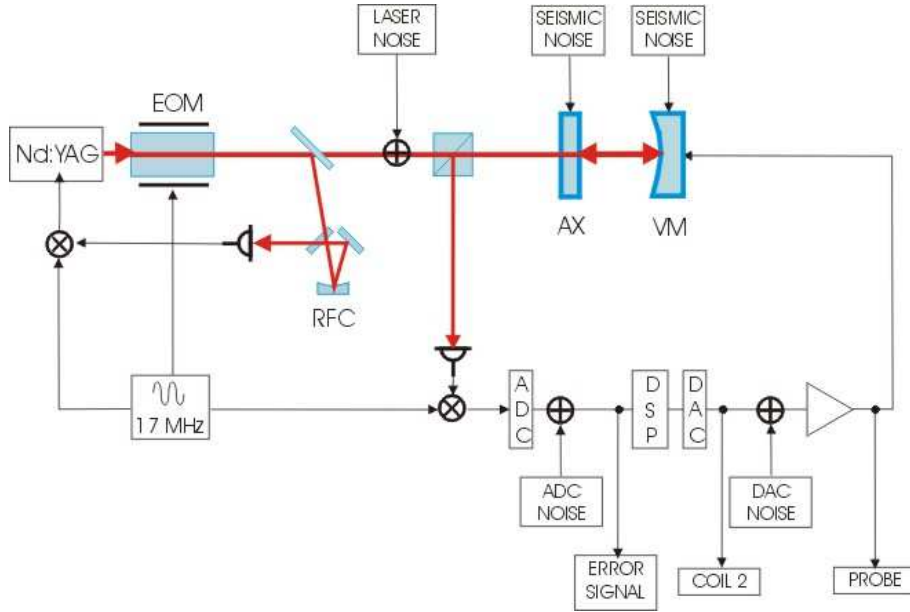


FIG. 3: Scheme of the control loop, which includes the main noise sources

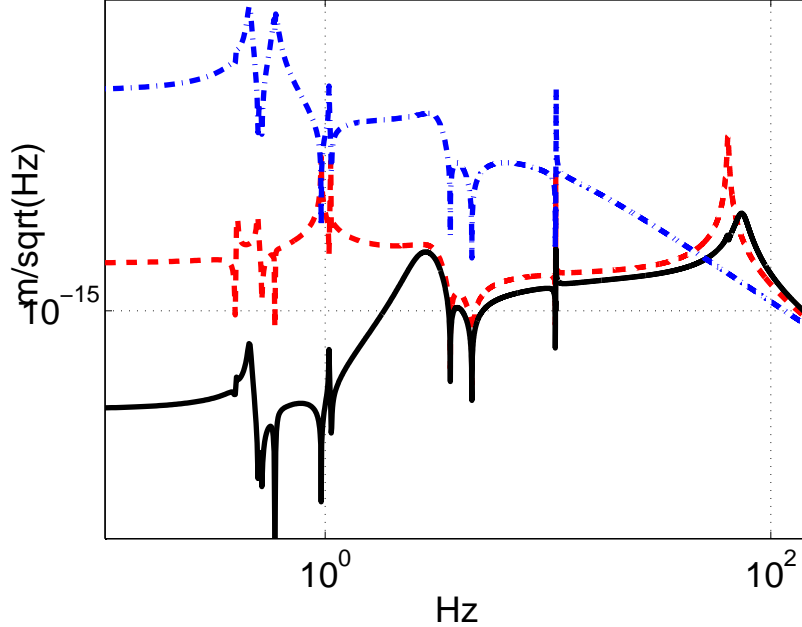


FIG. 4: Thermal noise power spectrum in the three cases: open feedback loop without optical spring (dot-dashed line) open feedback loop with optical spring (dashed line), closed feedback loop with optical spring (continuous line), typical LFF parameters are used.

the fact that the measurement is stationary, all not stationary noise sources (as Doppler shift due to the jitter of the injection beam, excited by seismic noise or by fluctuations of the air pressure induced by sound) are ruled out. As earlier mentioned, the different noise sources enter the system at different points, see fig. 3. While seismic noise enters only through the suspension, electronic noise

comes in through several ports: the laser (frequency and amplitude jitters), the mixer, the photodiode, the ADC, the DAC and the coil drivers. Direct measurement of the electronic noise has shown that the main contributions come from ADC and DAC. The electronic noise of the DAC and the driver cannot produce the measured spectrum. In order to produce a power spectrum similar

to the measured one, the noise of the DAC should be  $2 \times 10^{-4} \text{ V}/\sqrt{\text{Hz}}$ , which is more than a factor 100 higher than the measured DAC noise.

Signals are acquired just before the DAC (COIL2) and after at the level of the coil (PROBE, current flowing in the coil); the coherence of the signal COIL2 with the signal PROBE is very high, over 95% above 10 Hz: this confirms that the DAC noise is negligible.

Figure 5 shows the ratio between a noise injected before the DSP filter (as noise from the laser, mixer, photodiode and ADC noise) and the error signal; fig. 5 shows that a white noise would not reproduce the data in the frequency band 3 – 100 Hz.

In order to match the 80 Hz peak a noise with a spectral density of  $1.5 \times 10^{-3} \text{ V}/\sqrt{\text{Hz}}$  should be injected. on the other hand the ADC noise spectrum is white and its value is a factor 100 lower.

The frequency jitter of the Nd-YAG laser is one of the most important noise sources. For this reason, as we said before, we set -up a laser frequency stabilization loop which should limit the fluctuations at the  $\text{mHz}/\sqrt{\text{Hz}}$  level. However, since we haven't an independent reference cavity to perform a direct measurement of the residual noise, we have a strong evidence that this noise source does not contribute significantly to the noise floor of our set up. First all we notice that, in order to reproduce the measured power spectrum level around the optical spring resonance, we need a noise frequency jitter of  $\sim 350 \text{ Hz}/\sqrt{\text{Hz}}$ . This value is just a factor 5 below the measured laser frequency jitter in absence of stabilization. Moreover, we were able to evaluate an upper limit for the integrated frequency jitter with the following independent measurement. Before the runs, for calibration purposes, the P-D-H reflected signal was recorded, at 40 kHz acquisition rate, with the cavity out of lock. Each point taken in the linear region of the P-D-H signal has an error due to the frequency and amplitude jitter of the laser, and any other possible noise source, integrated from 0 to 20 kHz. Among all the recorded data an event has been selected, with over 30 points in the linear region: the cavity was moving slowly and with constant speed. Thirty six points have been recorded close to the linear region or the P-D-H signal, the data have been fitted with a polynomial up to ninth order. The difference between the points and the polynomial is a estimation of the noise affecting the measurement integrated from zero up to 20 kHz. The standard deviation of this noise is  $2 \times 10^{-4} \text{ V}$ , incompatible with a power spectrum density of  $1.5 \times 10^{-3} \text{ V}/\sqrt{\text{Hz}}$ . In figures 6 the data, the residuals of the fit are shown.

A detailed analysis of the seismic noise contamination can be found elsewhere [17]. Here we recall that the contamination of seismic noise at 10 Hz is below  $10^{-15} \text{ m}/\sqrt{\text{Hz}}$  for the VIRGO interferometer test masses.

## V. FIT RESULTS AND DISCUSSION

The study presented here is based on a set of data collected in different working conditions but with similar control loop gain and the test performed confirms compatibility of the data with the thermal noise prediction. As mentioned in a previous paragraph the most important signal used in our analysis is that related to the cavity de-tuning (closed loop error signal) obtained by reconstructing the signal output of the DSP (COIL2 in fig. 1). Indeed, this signal is acquired after a two poles Butterworth filter, which selects the frequency range 10 – 200 Hz. The region of the spectrum below 3 Hz is dominated by the seismic noise and it has been cut off by an other high pass filter applied to the data.

By means of the Horde software routine of the MatLab software package, we checked that data follow the Gaussian statistical distribution, while the data stationary has been checked by looking at the time-frequency spectrograms of the data.

According to the reference [2] an independent check of the data stationary for a thermal noise dominated system can be evaluated averaging the product between the speed and the acceleration of the observed system ( $\langle v_x \times a_x \rangle$ ,  $v_x$  and  $a_x$  are the speed and the acceleration). This parameter should vanish if the system is thermal noise dominated. The fig. 7 shows the distribution of the mentioned parameter (the average of the product between the speed and the acceleration of the system) averaged on increasing time interval and for frequencies below 100 Hz. The speed and the acceleration have been obtained differentiating the displacement measurements.

As stated by the Boltzman's law, the distribution of the speed ( $v_x$ ) for an oscillator excited by the thermal noise should be:

$$f(v_x) = \left( \frac{m}{2k_b T} \right)^{\frac{1}{2}} \times e^{-\frac{mv_x^2}{2k_b T}} \quad (3)$$

where  $m$  is the oscillator mass,  $k_b$  is the Boltzmann's constant and  $T$  the absolute temperature. Moreover, the variance  $\sigma$  of the distribution  $f(v_x)$  for a free oscillating system (not feedback controlled) is defined by the mechanical parameters. Our measurements have been performed with an active feedback loop which does not influence the distribution of the data but changes the absolute value of the variance itself. In principle the variance  $\sigma$ , for a closed loop case, could be reconstructed integrating the expected power spectrum all over the frequency band. The comparison between the measured spectrum and the predicted one, is the most reliable method to prove that the data are thermal noise dominated. Thus, we checked that the energy associated with the mirror AX, integrating the power spectrum between 3 and 100 Hz, is below  $k \times T/2$  ( $T \simeq 298 \text{ K}$ ).

Kubo in [2] states that for a system at the thermal equilibrium the admittance  $Y$  can be evaluated by the Fourier transform integrated from zero to infinity of the

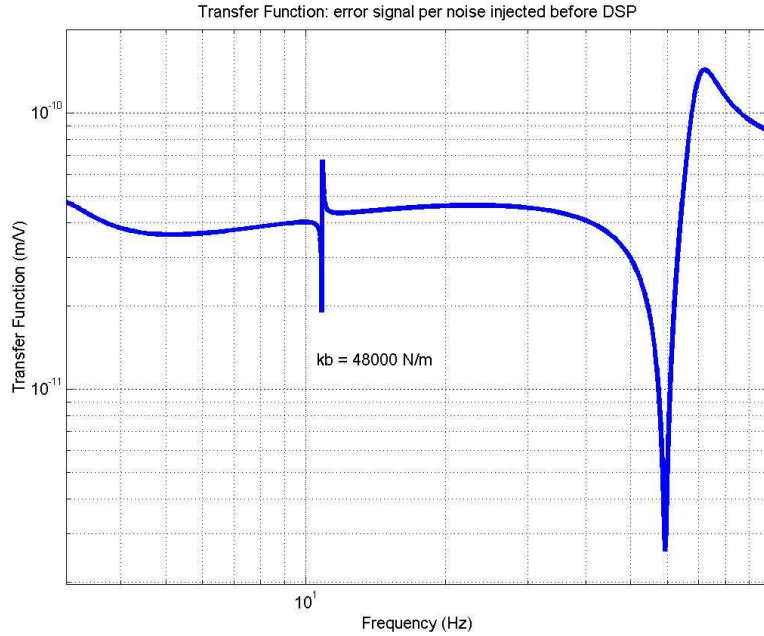


FIG. 5: PROBE Output versus frequency computed in the model by injecting a white noise before the DSP.

autocorrelation function of the speed. From the knowledge of  $Y$  it is possible to reconstruct the power spectrum from the fluctuation dissipation theorem. Let  $x_F$  be the displacement filtered by the feedback loops and by the filters of the acquisition system. The following relation held for the power spectrum of  $x_F$ :

$$S_{x_F x_F} = \frac{2}{\omega^2} \Re \left[ \int_0^\infty \left\langle \frac{dx_F(t+\tau)}{dt} \frac{dx_F(t)}{dt} \right\rangle e^{i\omega t} dt \right] \quad (4)$$

In fig. 9 we the  $S_{x_F x_F}$  is evaluated both directly from the data and applying the above equation. The agreement is good in particular in the region of the optical spring resonance and at higher frequencies. At lower frequency the stretch of data is too short to be used for deriving a significant estimation of the power spectrum on the base of the formula reported above. The good agreement shown is not sufficient to demonstrate that our measurements are thermal noise dominated. It represents just an efficient cross-check performed using uncalibrated and unfiltered data.

To evaluate the thermal noise contribution to the data we used our model to best fit the data. First all, we derived the absorption coefficient  $\gamma_l = 5.8 \text{ 1/s}$ , associated to the longitudinal motion of AX, by fitting the data selected around the optical spring resonance  $65 - 80 \text{ Hz}$ , while the other  $\gamma_\theta = 6.5 \text{ 1/s}$  is found by fitting the data in the interval  $3.5 - 6 \text{ Hz}$ , where there is the anti-resonance.

In the figure 8 we show the measured spectrum and the thermal noise contribution estimated by best fitting the data with the model for an optical gain  $1.56 \times 10^{10} \text{ V/m}$  and  $k_b = 56000 \text{ N/m}$ . Similar results have been obtained by analyzing the data of independent runs.

It has been also checked that present measurement is not compatible with the structural damping.

As it is shown in figure 8, the result of the fit and the data well agree below  $90 \text{ Hz}$ , at higher frequency the higher order modes are relevant, and the model cannot reproduce the data.

The mirrors are attached through wires, with diameter  $\phi = 300 \mu\text{m}$ , which in principle should be treated in the model as continuous system. The family of transversal modes of the wires (violin modes) starts around  $100 \text{ Hz}$ . It has been checked with the model that higher internal modes of the mirrors and violin modes of the wires, change the slope of the power spectrum above  $100 \text{ Hz}$ , and increases the level at lower frequency. The present set of data shows the power spectrum below  $200 \text{ Hz}$  and it is impossible to further constrain the model by adding higher order modes, since the high frequency resonance cannot be identified. As far as the frequency region below  $3 \text{ Hz}$  is concerned, we said before that we did not include in the model the super attenuator oscillation modes. However, a more detailed model would not improve the analysis, since this part of the spectrum is contaminated by seismic noise. We notice that the absorptions coefficients are about 10 times larger than those measured in VIRGO. The LFF apparatus is not as performing as VIRGO from the point of view of the losses due by mechanical dissipation. In fact, the LFF apparatus has not been constructed with all the care used for the VIRGO antenna; for example three wire loops are attached to the AX mirror, the wires diameter is rather large ( $300 \mu\text{m}$ ), the two wire loops holding the mirror are attached to a motor used to align horizontally the cavity.

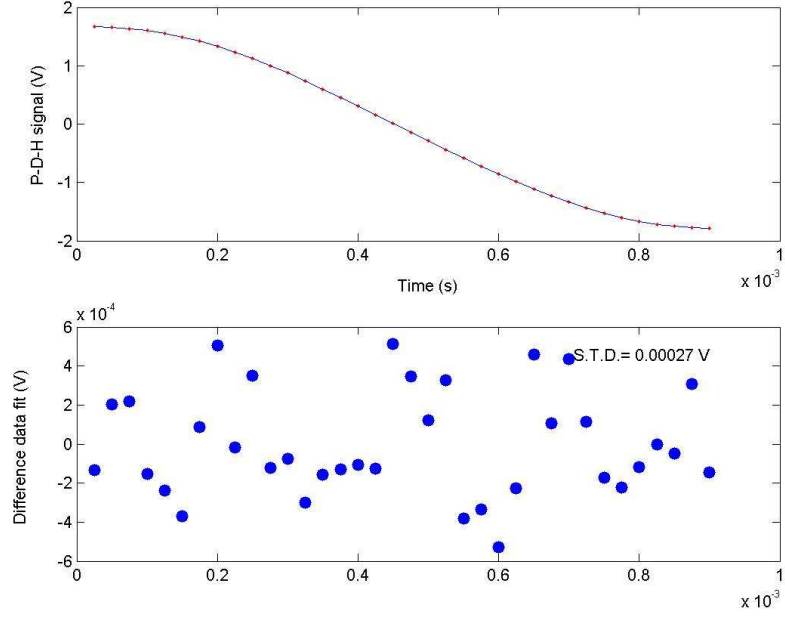


FIG. 6: up: P-D-H signal around the resonance, feed-back not active, over imposed is the the polynomial fit of the recorded points up to order 9.  
 down: difference measured points polynomial fit, which is a good measure of the noise coming from the laser, frequency and amplitude noise

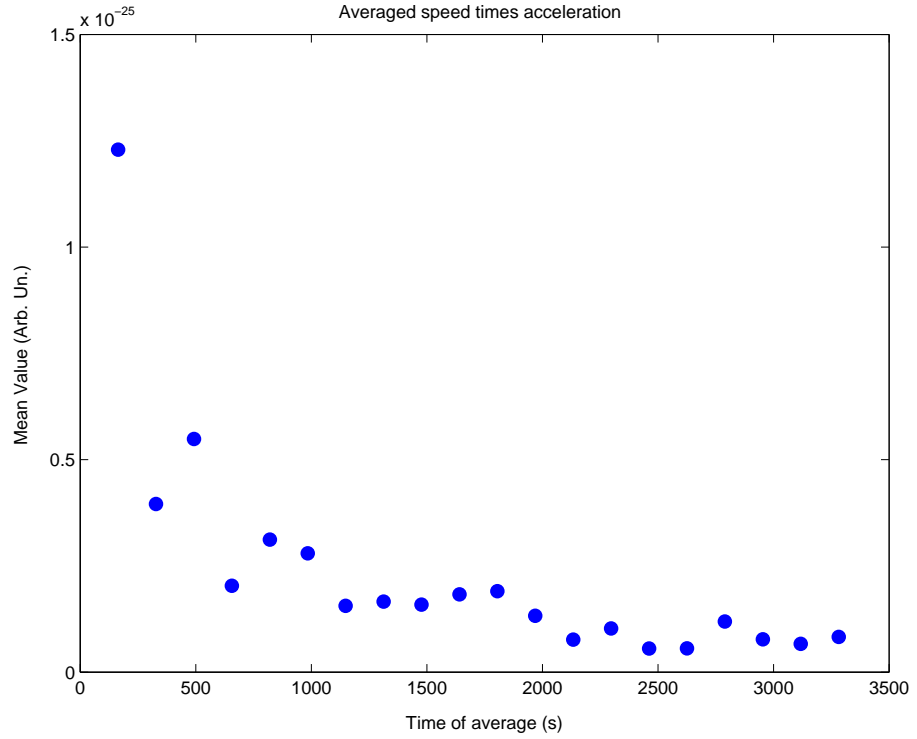


FIG. 7: Speed times acceleration averaged over time intervals of increasing length

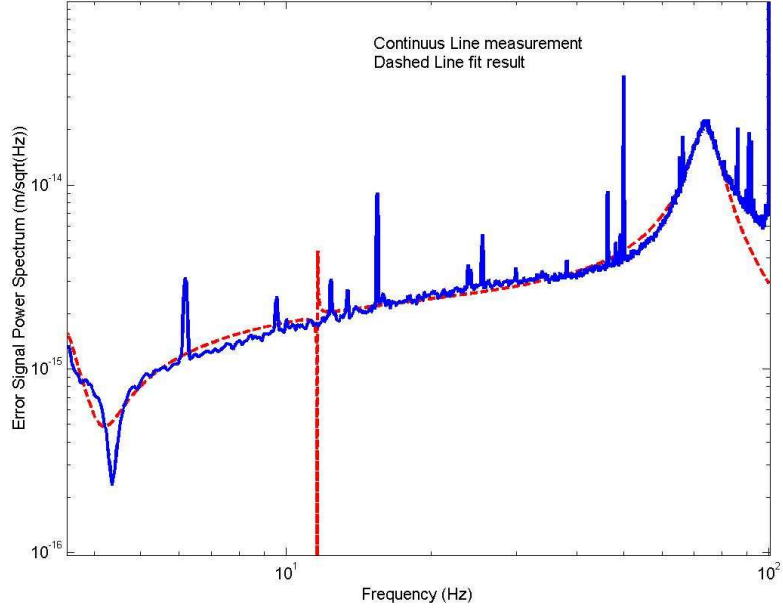


FIG. 8: Measured power spectrum,  $10 \text{ mHz}$  frequency resolution, compared with the thermal noise estimated by the model, assuming an optical gain  $1.56 \times 10^{10} \text{ V/m}$ ,  $k_b = 55000 \text{ N/m}$ , and the typical working conditions of the present set of runs, the losses, two parameters constant in frequency, are associated to the AM longitudinal and rotational degree of freedom, their fitted values are  $5.8 \frac{1}{\text{s}}$  for the longitudinal and  $6.5 \frac{1}{\text{s}}$

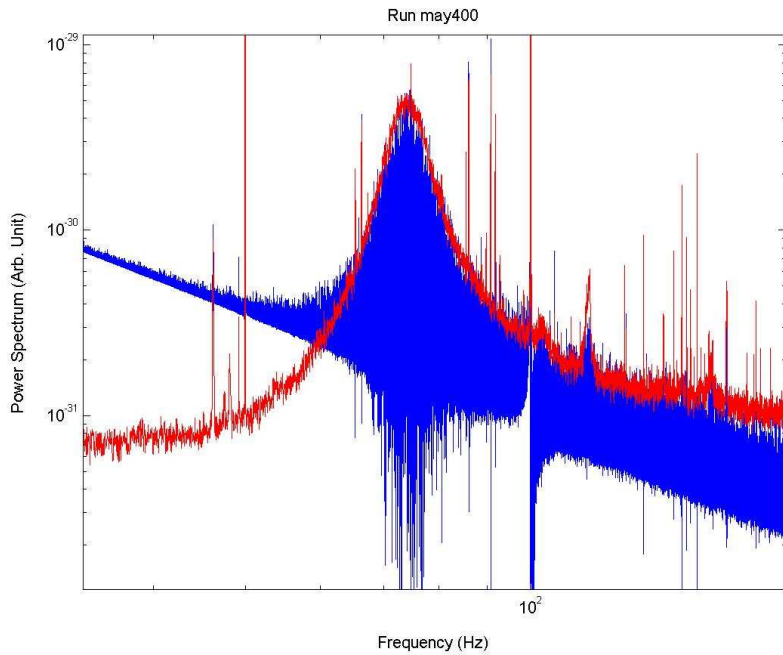


FIG. 9: Measured power spectrum compared with the power spectrum reconstructed by evaluating the admittance from the speed autocorrelation function and applying the Fluctuation Dissipation Theorem.

Due to the fact that the difference in length of the two wires loop, only 3  $mm$  apart, was causing a large vertical misalignment, it has been necessary to change the length of one of the two wires loops by using a clamp, which is attached directly to the wires of one of the two loops. This clamp consists of two pieces and a screw, which changes the distance between the two pieces, and accordingly the effective length of one of the two wires loop, thus making it possible to bend the AX mirror. In the model the losses are associated to the AX mirror motion, and the higher order mechanical modes of the system are not taken into account. Indeed we checked that higher order modes can contribute in decreasing the absorption coefficients.

Moreover, we notice that the the values of the two  $\gamma$  coefficients resulting from the data fit depend also on the absolute calibration: in particular they decrease when the optical gain is increased. For example, assuming a optical gain  $6 \times 10^{10} V/m$ , the fit gives  $\gamma_l = 0.13 1/s$  and  $\gamma_\theta = 1.06 1/s$ . The calibration of the LFF apparatus so far relies on measurements taken when the cavity feedback is off (open loop condition). The actuator system is calibrated applying a slowly increasing voltage to the coil drivers and we count the number of free spectral ranges transmitted by the cavity. In practice, the optical read out is calibrated by looking at the Pound-Drever signal; the two sidebands 34  $MHz$  apart, set the scale for the absolute calibration. In order to improve the calibration accuracy of the measurement, it would be necessary to have an independent system pushing the mirror of a know amount during the data taking based for example on the radiation pressure effect of an independent laser light, amplitude modulated at a fixed frequency impinging on the AX mirror. would move the AX mirror of  $10^{-14} m$ , at 20  $Hz$ , if the optical spring is  $64000 N/m$ . With the use of this calibrator it would be possible to directly excites the system for a direct measurement of the absorption mechanisms, on resonance and outside resonance.

## VI. CONCLUSIONS

A 1  $cm$  Fabry-Perot cavity is suspended using a super attenuator chain equal to the ones used for the VIRGO

antenna. This cavity has been locked for several hours, and the data analyzed off-line. The output signal exhibits a statistical behavior a displacement power spectrum compatible with the condition of a system at its thermal equilibrium. We developed a simple opto-mechanical model which include the various noise sources of the system and we evaluated the thermal noise contribution applying the fluctuation dissipation theorem. Two viscous dissipation coefficients  $\gamma_l$  and  $\gamma_\theta$ , constant in frequency, associated with the longitudinal and rotational motion of the lighter test mass of 0.350  $kg$ , are used in the model to fit the data; the fit results gives  $\gamma_l = 5.8 1/s$  and  $\gamma_\theta = 6.5 1/s$ . Different runs give similar results. In particular the measured power spectrum is reproduced in the region 3 – 90  $Hz$  under the hypothesis that it is thermal noise dominated. We checked that the measured power spectrum cannot be produced by external noise sources, as noise of the laser and electronics and that the other noise source in the control loop are not contributing significantly.

## Acknowledgements

We would like to thank all the technicians of the Pisa-INFN sections, who have contributed to the construction of the LFF experiment: R. Cosci, C. Magazzu', A. Di Sacco, A. Del Colletto, F. Mariani, and M. Iacoponi. We thank M. Perciballi and M. Iannone of Rome, P. Dominici of Urbino and S. Di Franco of Florence. Special thanks goes to M. Ciardelli, R. Macchia, F. Nenci and A. Pasqualetti, now working for EGO.

## References

---

- [1] JK. Thorne, gr-qc/9704042 and B. Shutz, Clas. Quan. Grav., 16, 1999, A131-A156.
- [2] R Kubo 1966 Rep. Prog. Phys. 29 255-284
- [3] Callen H.B. And Welton T.A. , Phys. Rev. 83 34-40
- [4] P. Saulson, Phys. Rev. D 42, 2437 (1990).
- [5] K. Yamamoto et al., Class Quant. Grav. 19 (2002) 1689-1696.
- [6] M. Gonzales and P. Saulson, J. Acoust. Soc. Am. 96, 207-212 (1994).
- [7] Numata et al., Phys. Rev. Lett. 91 (26), 260602 (2003).
- [8] Courty et al., Phys. Rev. Lett., 90, 83601-1-4 (2003).
- [9] A. Di Virgilio et al., J. Physics: Conference Series, Vol. 32 (2006), 346-352.
- [10] A. Di Vigilio et al., Phys. Rev. A, 74, 13813 (2006);
- [11] G. Ballardin et al., Rev. Sci. Instrum., **72**, 3643 (2001).
- [12] G. Losurdo et al., **72**, 3654-3661 (2001).
- [13] M. Bernardini, E. Majorana, P. Puppo, P. Rapagnani, F. Ricci, G. Testi, Rev. Sci. Instrum., **70**, 3463 (1999).
- [14] VIRGO Collaboration, VIRGO Physics Book, Optics and related Topics, Chap. II. Can be downloaded from

<http://www.VIRGO.infn.it/>

[15] N. A. Robertson et al., *Class. Quant. Grav.* 19, 4043-4058 (2002).

[16] Cagnoli et. al, *Phys. Lett. A* 213, 245-252 (1996).

[17] A. Di Virgilio, *VIRGO Note*, VIR-NOT-PIS-1390-334